Antibacterial copper-doped calcium phosphate glasses for bone tissue regeneration

Farzad Foroutan, [a,+] *Jamie McGuire,* [a,+] *Priyanka Gupta,* [b] *Athanasios Nikolaou,* [a] *Benjamin A. Kyffin,* [a] *Nicole L. Kelly,* [c] *John V. Hanna,* [c] *Jorge Gutierrez-Merino,* [d] *Jonathan C. Knowles,* [e,f,g,h] *Song-Yi Baek,* [e] *Eirini Velliou,* [b] *Daniela Carta* [a *]

[a] Department of Chemistry, University of Surrey, GU2 7XH, Guildford, UK.

[b] Department of Chemical and Process Engineering, Bioprocess and Biochemical Engineering group (BioProChem), University of Surrey, Guildford, UK.

[c] Department of Physics, University of Warwick, Coventry, CV4 7AL, UK.

[d] School of Biosciences and Medicine, University of Surrey, Guildford, GU2 7XH, UK.

[e] Division of Biomaterials and Tissue Engineering, University College London, Eastman Dental Institute, 256 Gray's Inn Road, London WC1X 8LD, UK.

[f] The Discoveries Centre for Regenerative and Precision Medicine, UCL Campus, London, UK.

[g] Department of Nanobiomedical Science & BK21 PLUS NBM Global Research Center for Regenerative Medicine, Dankook University, Cheonan 31114, Republic of Korea.

[h] UCL Eastman-Korea Dental Medicine Innovation Centre, Dankook University, Cheonan 31114, Republic of Korea.

[*]Corresponding author: d.carta@surrey.ac.uk

+ These authors have equally contributed to this work.

KEYWORDS: Calcium phosphate glasses, bone regeneration, controlled ion release, antibacterial activity.

ABSTRACT

Calcium phosphate glasses are a promising new generation of biomaterials that can simultaneously induce tissue regeneration and controlled release of therapeutic molecules. In this work, novel calcium phosphate glasses containing 0, 2, 4 and 6 mol% Cu^{2+} were synthesised via room temperature precipitation reaction in aqueous solution. The effect of Cu^{2+} addition on the glass properties and structure was investigated using thermal analysis, ^{31}P solid state MAS NMR, Raman spectroscopy and X-ray diffraction. All glasses crystallise at temperature >500 °C and are mainly formed by Q^1 groups. The release of P, Ca and Cu in solution over time was monitored via inductively coupled plasma-optical emission spectroscopy. It was found that with increasing Cu content, the amount of P and Ca released decreases whereas the amount of Cu released increases. The effect of Cu^{2+} release on the antibacterial activity against *S. aureus,* a bacterial strain commonly found post-surgery infections, has been investigated. The addition of copper has been shown to infer the glasses antibacterial properties. As expected, the antibacterial activity of the glasses increases with increasing Cu^{2+} content. Cytocompatibility was assessed by seeding human osteoblast-like osteosarcoma cells Saos-2 (HTB85) on the glass particles. A significant increase in cell number was observed in all the glasses investigated. The copper-doped calcium phosphate glasses have proven to be multifunctional, as they combine bone regenerative properties with antibacterial activity. Therefore, they have great potential as antibacterial bioresorbable materials for hard tissue regeneration.

1. INTRODUCTION

Calcium phosphate glasses have been subject of increased interest in recent years due to their potential application in the regeneration and repair of hard and soft tissues. [1, 2] They can be defined as bioresorbable, as they are able to interact with the physiological fluids producing the desired biological response and simultaneously dissolve completely over time being eventually entirely replaced by regenerated tissue. [3] Thanks to their complete solubility, they can be used as safe degradable temporary implants, avoiding the necessity of a second operation for their surgical removal. [4] Moreover, they can be used as controlled local delivery systems of therapeutic molecules (e.g. antimicrobial ions/growth factors) that will be slowly released as the implant degrades. [5] In particular, the addition of antimicrobial ions prevents biomaterial-related infections which often cause revision surgery. Their controlled delivery will avoid the systematic conventional administration treatments (oral and injection) which usually require higher doses of drugs that can cause toxic reactions. Currently, the most common bioresorbable materials are polymers (*e.g.* polylactic and polyglycolic acid). However, their degradation often results in crystalline fragments that could lead to toxicity. [6] Differently from the polymer-based bioresorbable systems, phosphate-based glasses do not release any crystalline products which could lead to inflammation. Phosphate-based glasses also present a great advantage over silicate-based glasses which have a very slow solubility and therefore can only be used to manufacture long-term implants which are susceptible to long-term failure/inflammatory reactions. In addition, dissolution rate and ion release can be controlled and tailored according to the desired application by altering the glass composition. [7] The most common method to prepare calcium phosphate glasses is using a conventional melt-quenching (MQ) technique that requires melting of oxide powders at temperatures >1100 °C and rapid cooling. [8] However, this method often leads to non-

homogeneous glasses and loss of phosphorus. More recently, the sol-gel (SG) route has been proposed as an alternative technique for the synthesis of phosphate glasses. [9-13] However, phosphorous precursors (typically alkoxides) used in the sol-gel process are air-sensitive and need to be dissolved in organic solvents. Moreover, gelation time can vary from few hours to days. Recently, a room temperature, water-based technique for the synthesis of undoped calcium pyrophosphate glasses was presented. [14, 15] In this work we have used this single step precipitation technique to synthesise a series of copper-doped calcium phosphate glasses containing 0, 2, 4 and 6 mol % Cu^{2+}. To date, copper-doped phosphate glasses have only been prepared via MQ. [16] In the very few papers published on the topic, copper has been shown to infer MQ phosphate-based glasses antibacterial property as the glasses degrade. [17-19] When addedd to silicate-based glasses, copper has also shown promotion of osteogenesis and angiogenesis [20] and increase in differentiation of mesenchymal stem cells towards the osteogenic lineage, [21] in addition to antibacterial activity against *Escherichia coli.* [22] In the present work, we have investigated antibacterial activity of copper-doped calcium phosphate glasses against *Staphylococcus aureus (S. aureus)*, one of the most common pathogen associated with orthopaedic device-related infections and also associated with antibiotic resistance. [23]

Bioresorbable calcium phosphate glasses find mainly applications in bone tissue regeneration as their composition is very similar to the bone. [2] New bone formation is stimulated through the release of P and Ca when the implant is exposed to an osseous defect. Previous *in vitro* cytocompatibility studies have been presented on the growth of bone cells on phosphate-based glasses prepared via MQ: human osteosarcoma derived cell lines MG63 [6, 24-26], HOS [26, 27], primary-derived human osteoblasts [28] and craniofacial osteoblasts. [29] However, no previous works have been presented on the cytocompatibility of calcium phosphate glasses prepared via in

solution, water based techniques. The present study has therefore investigated the biocompatibility of a series of copper doped calcium phosphate glasses on the attachment and proliferation of the osteoblast-like cell line Saos-2 (HTB85) and the effect of addition of Cu^{2+} on the biocompatibility of the glasses.

2. MATERIALS AND METHODS

2.1. Synthesis

Amorphous calcium phosphate glasses were prepared using a method adapted from Slater *et al.* [30] 50 mL of 1 M calcium chloride dihydrate ($CaCl_2.2H_2O$, Sigma Aldrich, 97%) solution was added to a 50 mL solution of 0.2 M potassium pyrophosphate ($K_4P_2O_7$, Sigma Aldrich, 97%) at a flow rate of 2 mL/min under vigorous stirring. The solution was then filtered via Buchner funnel immediately after addition of the $CaCl_2$ solution. The precipitate was then washed twice, first with deionised water, then ethanol. The precipitate was then allowed to dry in air for two days. Copper-doped calcium phosphate glasses were synthesised by addition of 50 mL of $Cu(NO_3)_2$ (Acros Organics, 99%) to the $CaCl_2$ solution at different concentrations such that the total mol% Cu^{2+} was equal to 2, 4 and 6 mol%. The moles of $CaCl_2$ were reduced to compensate for the addition of the $Cu(NO_3)_2$. This mixture was then added to the potassium pyrophosphate solution as previously described. In order to investigate the stability of the glasses under thermal treatment, calcination was performed at 200, 400 and 700 °C in air using a heating rate of 1 °C/min. The obtained glasses were ground at 10 Hz to form microparticles and then sieved (Endesotts Ltd, London, UK) to obtain particles in the size range of 200-300 μm. Samples will be hereafter indicated as CPG (undoped) and CPG_CuX (doped) where CPG stands for calcium phosphate glasses and X indicates the mol% of Cu^{2+}.

2.2. Characterisation

Structural characterisation and chemical analysis

Scanning Electron Microscopy (SEM) was performed with a JSM-7100F, Jeol field emission electron microscope. A fixed accelerating voltage of 15 kV was used with variable probing currents. Samples were mounted on aluminium sample holders using graphite paste and coated with graphite.

Energy Dispersive X-ray spectroscopy (EDX) was performed using a WDS MagnaRay Spectrometer was performed to determine the exact compositions of the prepared samples. SEM was operated at 20 kV, spot size 6 and a working distance of 10 mm.

X-ray diffraction (XRD) was performed using PANalytical X'Pert on samples in a flat plate geometry using Ni filtered Cu Kα radiation (λ = 1.5418 Å). Data was collected using a PIXcel-1D detector with a step size of 0.05 ° over an angular range of 2θ = 10-90° and a count time of 12 s per step.

Simultaneous thermogravimetric analysis (TGA) and *differential scanning calorimetry (DSC)* were performed on a TA Instruments-SDT Q600 in air in the range 25 °C - 1000 °C at a heating rate of 10 °C/min in an alumina crucible.

^{31}P magic angle spinning solid-state nuclear magnetic resonance (MAS NMR) data were acquired at ambient temperature (~25 °C) using a Bruker AVANCE III-500 spectrometer operating at a ^{31}P Larmor frequency of 202.46 MHz. All measurements were facilitated using a Bruker 4 mm dual channel HX probe MAS frequencies of 12 kHz for this study. These ^{31}P MAS NMR data were acquired using single pulse (direct detection) methods and the pulse calibration and chemical shift referencing was performed using solid the secondary reference ammonium dihydrogen phosphate ($NH_4H_2PO_4$, δ 0.9 ppm) with respect to the IUPAC primary reference of 85% H_3PO_4 (δ 0.0 ppm).

An π/2 excitation pulse of 3 μs and a recycle delay of 60 s were used in all experiments; this relaxation delay was checked against longer recycle delays to ensure full spin-lattice (T_1) relaxation. Between 20 and 88 transients were acquired for each measurement, and all spectra were simulated using the Dmfit software package. [31]

Raman spectroscopy was performed on a DXR™, Thermo Fisher Scientific at a 532 nm using a 10 mW power beam laser in the range of 1400-200 cm^{-1}.

2.3. Dissolution study

In order to assess the species released upon dissolution, 10 mg of each glass composition were immersed in 10 mL deionised water for 1, 3, 5, and 7 days with three replicates for each conditions (n=3). The resulting suspensions for each time points were then centrifuged at 4800 rpm for 10 min to separate the glass particles from the solution. Calcium, phosphorus, and copper in solution were subsequently measured by inductively coupled plasma-optical emission spectroscopy (ICP-OES 720ES, Varian) calibrated across the predicted concentration range using a standard solution (ICP multi-element standard solution, VWR). Both samples and standards were diluted 1:1 in 4% HNO_3 (Fluka) and analysed in reference to a blank (2% HNO_3) solution under standard operating conditions.

2.4. Antibacterial studies

The bactericidal effect of the synthesised glasses was determined using the quantitative Agar Dilution Method (ADM) as described by Gutierrez *et al*. [32] Universal tubes with 10 mL Tryptic Soy Broth (TSB) were inoculated with 100 mg of each glass powders and an overnight culture of *S. aureus* at 10^6 CFU/mL. The *S. aureus* strain used was recently isolated and sequenced as

reported by Stedman *et al.* [33] sharing a 99% of identity with the standard strain NCTC 7447. Tubes were incubated at 37 ºC for 1 week at 250 rpm and samples were collected after 1, 3, 5 and 7 days to calculate viable CFU/mL of *S. aureus* for each time point. The overnight bacterial cultures were obtained in TSB at 37 ºC for 24 hours, at 250 rpm and the experiments were conducted as two biological replicates; the glass containing no copper was used as negative controls.

2.5. Cytocompatibility Assessment

2.5.1. Cell culture

Saos-2 (HTB85), osteosarcoma cells were procured from ATCC and cultured in McCoy's 5a medium (ATCC) with 15% fetal bovine serum (FBS, Gibco, Invitrogen) and 1% antibiotic-antimycotic (Thermo Scientific) in a humidified incubator at 5% CO_2 and 37 °C. On reaching 90% confluency, cells were passaged and used for cytocompatibility analysis for the materials. To facilitate the attachment of the cells on to the materials, polycarbonate cell culture inserts with 0.4 µm pore size (Merck Millipore) was used. Materials were placed on the inserts and incubated with medium overnight. 1.2 $x10^4$ cells were placed in each insert with the different materials and cultured for 5 days with cell viability assessment during the culture period. Cells only on inserts was used as control for comparison purposes.

2.5.2. Cell attachment and growth

SEM was used to visualise cell attachment and growth on glass surfaces. At the end of day 5, cells were fixed with 3% glutaraldehyde (Sigma-Aldrich) followed by dehydration using graded ethanol. Samples were then air dried, gold sputter coated and visualised using JSM7100F, Jeol scanning electron microscope.

2.5.3. Alamar Blue cell viability assay

Alamar Blue assay was carried out on days 1, 3 and 5 to assess cell viability and growth. Cells were incubated for 2 hours in a 10% Alamar Blue solution (ThermoFisher) followed by fluorescence measurement with a BioTek plate reader at 530 nm excitation and 590 nm emission as a direct estimation of cell growth on the different materials.

2.5.4. DAPI- Phalloidin staining

At the end of day 5, the cells were fixed using 4% paraformaldehyde and stained with DAPI-Phalloidin for visualisation of the nucleus and actin filaments. Cells were incubated for 20 mins at room temperature in staining solution containing 2.5µl of DAPI (1mg/ml stock solution, Thermo Scinetific), 4µl of Phalloidin (200 U/ml stock concentration, Alexa Fluor 488, Phalloidin, Life Technologies) and 20µl of Triton X per ml of PBS. Cells were then visualised using Cytation5 Cell Imaging Multimode Reader (Biotek).

3. RESULTS

3.1. Assessment of glass composition

Chemical analysis of the samples was carried out using SEM equipped with EDX detector. Elemental compositions in terms of weight% and mol% are reported in **Table 1**. The Ca/P of the undoped sample is equal to 1.0 and it corresponds to the pyrophosphate stoichiometry. This is in agreement with the synthesis used which was designed to produce calcium pyrophosphate glasses. [30] The Ca/P ratio decreases as the copper content increases as expected given that the calcium was replaced with copper in the synthesis. Therefore, as expected, in the doped samples, the Ca amount decreases as the copper amount increases. The Ca/P molar ratio, which varies between 1.0 and 0.5 is in agreement with the Ca/P molar ratio found in the majority of calcium phosphate phases of biomedical interest which varies between 1.0 and 0.5. [34] It has to be noted that a small amount of

potassium is also present in all glasses. Residual potassium was also found in undoped calcium pyrophosphate glasses prepared with the same synthetic protocol. [35]

Table 1. Compositions of the glasses measured by EDX

Sample	Element weight%					Element mol%					
	P	Ca	K	Cu	O	P	Ca	K	Cu	O	Ca/P
CPG	20.9	28.5	3.3	-	47.3	15.2	16.1	1.9	-	66.8	1.0
CPG-Cu2	19.9	22.1	3.1	6.2	48.6	14.6	12.5	1.8	2.2	68.9	0.9
CPG-Cu4	20.9	21.4	2.6	12.0	43.2	16.2	12.8	1.6	4.5	64.9	0.8
CPG-Cu6	18.9	13.3	2.6	17.2	48.1	14.3	7.7	1.6	6.3	70.1	0.5

A representative EDX spectrum used to calculate the elemental compositions and a representative EDX chemical map used to evaluate distribution of all elements are shown in **Figure 1A** and **1B**, respectively. The EDX map shows that the distribution of all elements on the surface of the glass particles is highly homogeneous, including the dopant copper.

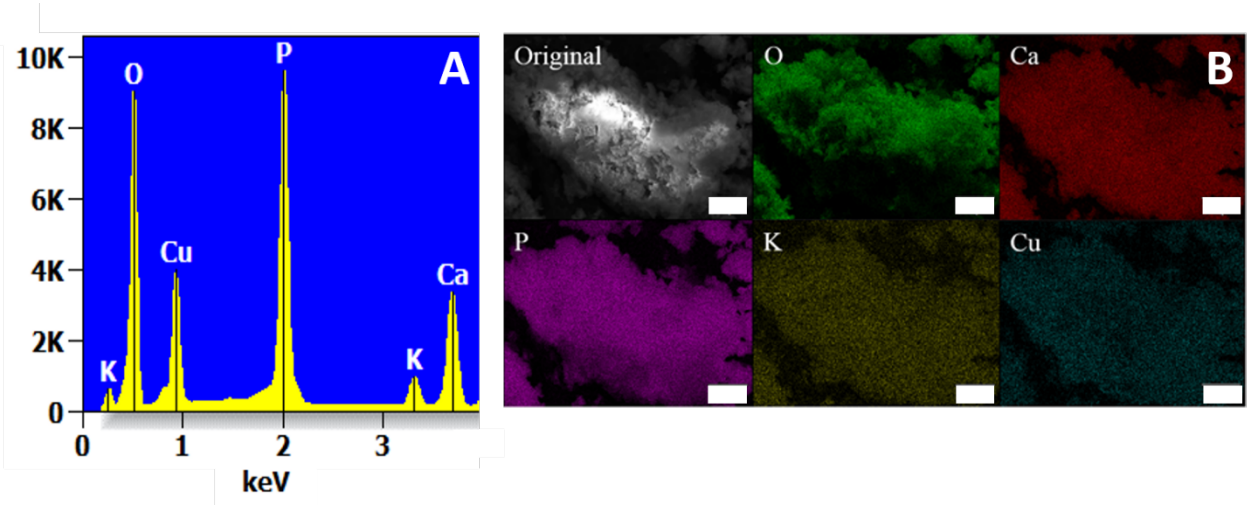

Figure 1. A) EDX spectrum and B) EDX mapping of the representative sample CPG-Cu6. Scale bar is 10 µm.

3.2. Thermogravimetric Analysis

Weight loss of all glasses and identification of thermal events upon heating were assessed using simultaneous differential scanning calorimetry (DSC) and thermogravimetric analysis (TGA). TGA and DSC curves are shown in **Figure 2** and main weight losses and crystallisation temperatures are reported in **Table 2**. All samples exhibit one main weight loss (16.8-20.0 %) between 25 °C and 150 °C. This event, which corresponds to a broad endothermic peak in the DSC trace, can be ascribed to dehydration of the sample. The total weight loss is similar for all the Cu^{2+} doped samples (about 20 %) and slightly higher for the undoped glass (about 24 %). A single sharp exothermic peak is observed between 533 °C and 625 °C in all samples, ascribed to the crystallisation of the glass.

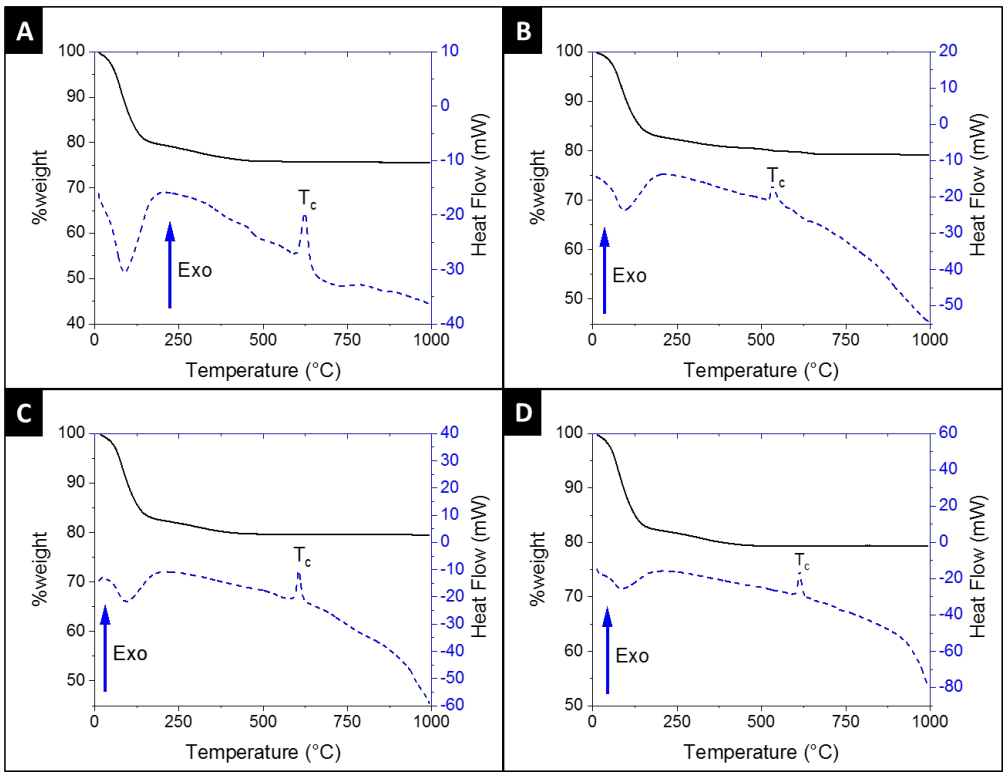

Figure 2. TGA (dotted line) and DSC (solid line) of A: CPG; B: CPG-Cu2; CPG-Cu4; CPG-Cu6.

Table 2. Weight loss % and crystallization temperatures (T_c) obtained from TGA and DSC plots.

Sample	Weight loss % in the range 25-150 °C	Total weight loss %	Tc (°C)
CPG	20.0	24.3	625
CPG-Cu2	17.0	20.8	533
CPG-Cu4	16.8	20.5	606
CPG-Cu6	17.0	20.7	614

3.3. X-ray diffraction

XRD patterns of all samples, reported in **Figure 3**, clearly show absence of Bragg peaks indicating that all samples are amorphous. The only feature observed is the broad halo around 28° which is due to the amorphous phosphate network. Therefore, the introduction of Cu^{2+} even up to 6 mol % does not induce crystallisation. In order to assess the thermal stability, glasses were then calcined at 200, 400 and 700 °C. As shown in **Figure S1**, the XRD patterns of all samples calcined up to 400 °C are still amorphous. However, after calcination at 700 °C, fully crystallisation occurs with formation of calcium pyrophosphate α-$Ca_2P_2O_7$ (ICDD card 09-0345). XRD results are in fully agreement with the DSC results as Bragg peaks are evident only in the samples calcined at 700 °C.[36]

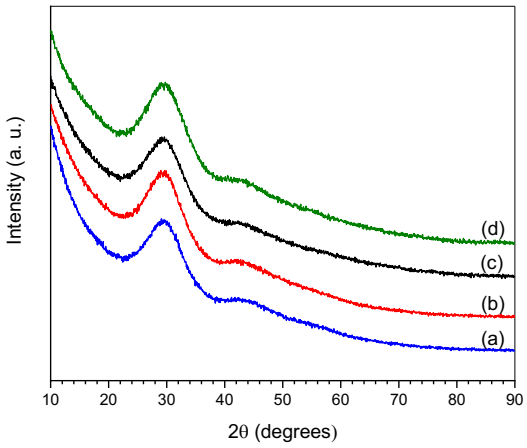

Figure 3. XRD patterns of: (a) CPG; (b) CPG-Cu2; (c) CPG-Cu4; (d) CPG-Cu6.

3.4. ^{31}P MAS NMR

The ^{31}P MAS NMR technique was used to characterise the local environment around each phosphorus species. The ^{31}P MAS NMR data presented in **Figure 4** show resonances that are assigned to Q^n groups, where n represents the number of bridging oxygens between phosphate units. Spectral parameters are presented in **Table 2**. In all samples, the predominant resonance is located at a chemical shift of ~ –6 ppm which is typical of the Q^1-type pyrophosphate unit ($P_2O_7^{4-}$). [37] A contribution from Q^0 groups which is attributed to isolated tetrahedral orthophosphate (PO_4^{3-}) units is also observed in all samples in the chemical shift range of ~ -2.8 – 1.8 ppm. The presence of Q^0 groups can be ascribed to the partial hydrolysis of some of the pyrophosphate ions during the synthesis of CPG or to PO_4^{3-} units contained in the precursors during the synthesis. [30, 38] From **Figure 4** it can be observed that only Q^0 and Q^1 groups are observed to constitute the CPG and CPG-Cu2 systems; however, CPG-Cu4 and CPG-Cu6 show an additional resonance at around −16 ppm which is ascribed to the formation of polymeric -P-O-P- (Q^2) groups. From the compositions of these systems outlined in **Table 1**, an increase in copper content coincides with a marked decrease in network modifying Ca speciation thus leading to the formation of some polymeric -P-O-P- (Q^2) groups. It is unlikely that this observed shift corresponds to a -Cu-O-P- linkage as the strongly paramagnetic Cu^{2+} species would broaden the nearby P position beyond detection. Indeed, not all of the P speciation will be observed in the ^{31}P MAS NMR experiment as those positons proximate (*i.e.* nearest neighbour) to the introduced Cu^{2+} species will paramagnetically broadened beyond detection; this phenomenon becomes more prominent as the copper content increases. From **Figure 4** the relative intensity of Q^n groups changes with increasing Cu^{2+} content and a concomitant decreasing Ca^{2+} content. The undoped CPG sample exhibits a predominance of Q^1 groups (integrated intensity of ~98%) is in agreement with the pyrophosphate stoichiometry

confirmed by the Ca/P ratio calculated using EDX results, with only ~ 2 % of the P speciation in this sample being comprised of Q^0 units. The CPG-Cu2 system shows that the relative intensity of Q^1 groups decreases to ~ 84 %, with the remaining ~ 16 % of the P speciation represented by Q^0 units. However, the CPG-Cu4 and CPG-Cu6 systems exhibit the onset of Q^2 formation as the relative intensity of the Q^1 groups decreases to 63.9 and 43.5 %, respectively.

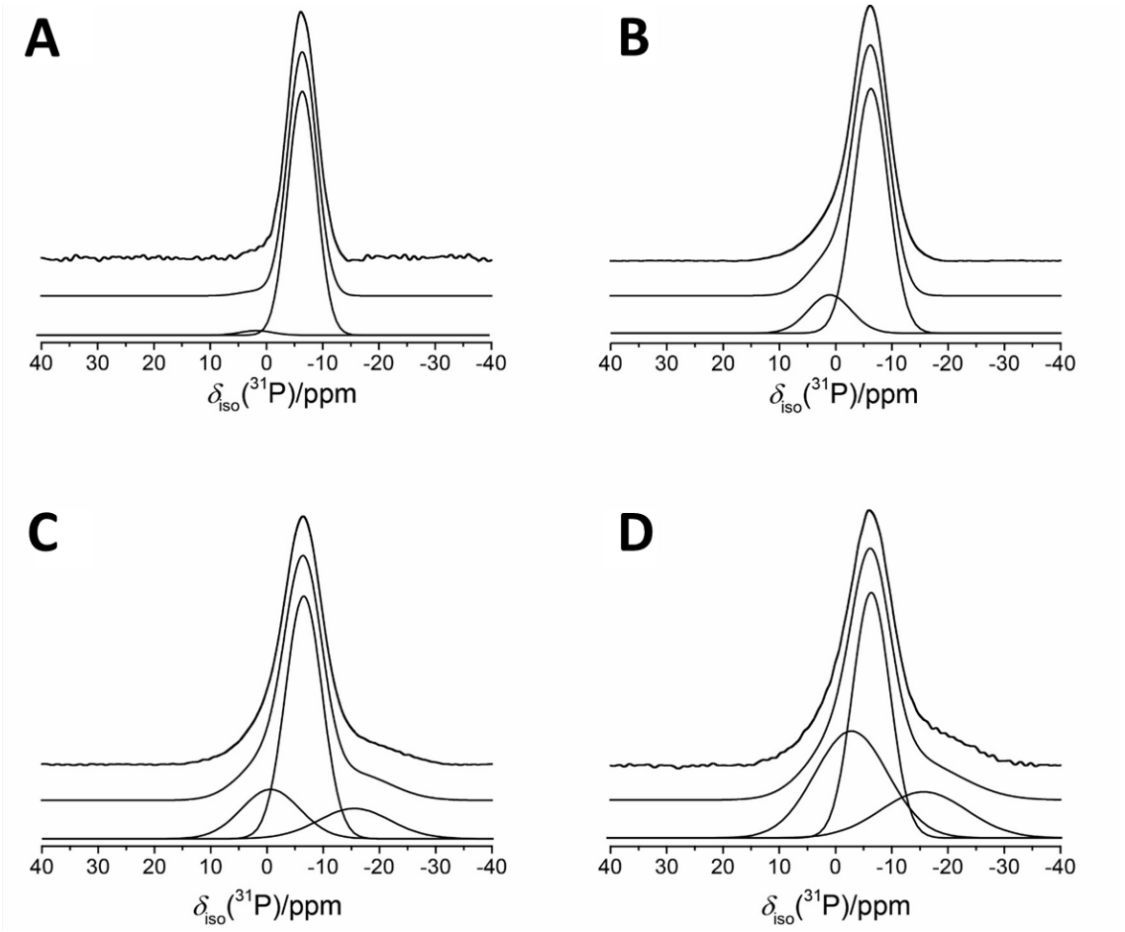

Figure 4. ^{31}P MAS NMR spectra of A) CPG; B) CPG-Cu2; C) CPG-Cu4; D) CPG-Cu6. The lines from top to bottom are: raw NMR signal, smoothed curve and deconvoluted peaks.

Table 2. ^{31}P MAS NMR spectral parameters (chemical shift, δ_{iso}) and relative intensity (I %)) obtained by signal deconvolution achieved using the DMFit post-processing programme.

	Q^0		Q^1		Q^2	
	δ_{iso} (ppm)	I %	δ_{iso} (ppm)	I %	δ_{iso} (ppm)	I %
CPG	1.8	2.1	− 6.4	97.9		
CPG-Cu2	1.0	16.0	− 6.3	84.0		
CPG-Cu4	− 0.6	20.6	− 6.5	63.9	− 15.5	15.5
CPG-Cu6	− 2.8	37.1	− 6.4	43.5	− 15.7	18.9

3.5. Raman spectroscopy

Raman spectra of all glasses are presented in **Figure 5**. All bands are quite broad confirming the amorphous nature of all samples. Bands in the frequency region between 200 and 950 cm^{-1} arise from vibrations of the in-chain P-O-P bonds, whereas bands in the frequency region between 950 cm^{-1} and 1400 cm^{-1} arise from out-of-chain $(PO_3)^{2-}$. [39] The predominant bands which occur at 770 cm^{-1} and 1050 cm^{-1} are typical of short chain Q^1-type pyrophosphate ($P_2O_7^{4-}$) in agreement with ^{31}P MAS NMR data. They can be assigned to the symmetric stretching mode of P-O-P in very short chains and $(PO_3)^{2-}$ terminal groups, respectively. [40] Typical bending vibrations of a network structure dominated by pyrophosphate groups are observed in the range 480-650 cm^{-1}. [41, 15] Another significant band occurs at 340 cm^{-1} which is due to bending of $(PO_4)^{3-}$ units linked to Ca^{2+} and/or Cu^{2+} as cation modifiers. [42] The broad band at 1190 cm^{-1} can be attributed to asymmetric stretching motions of the $(PO_3)^{2-}$ groups. [15] This band becomes more prominent as the Cu^{2+} content increases, in agreement with similar zinc doped MQ phosphate glasses.[39] The band at 930 cm^{-1} is due to asymmetric stretching of P-O-P.

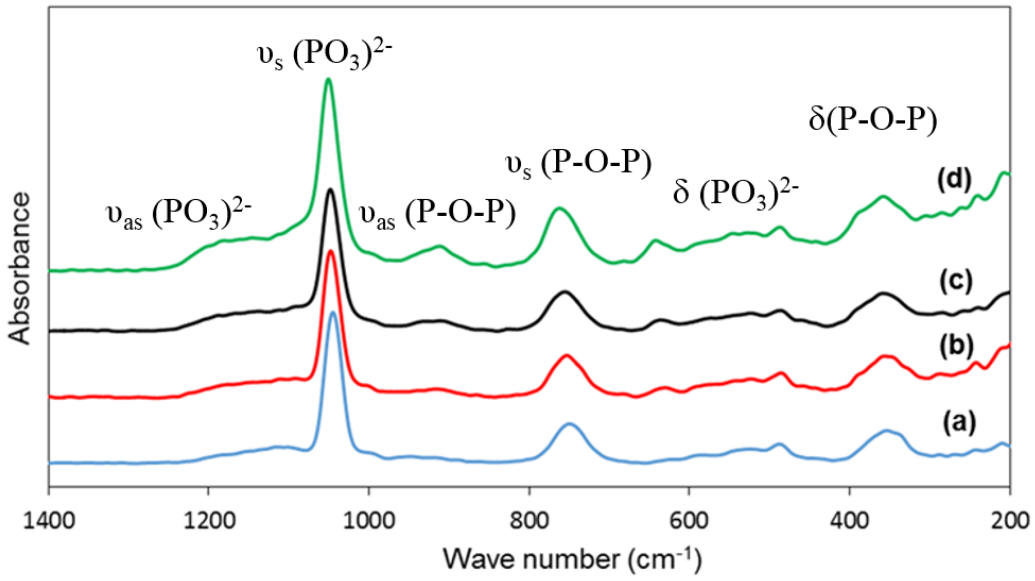

Figure 5. Raman spectra of (a) CPG; (b) CPG-Cu2; (c) CPG-Cu4; (d) CPG-Cu6.

3.6. Dissolution study

The concentrations of phosphorus, calcium, and copper released in water at different time points up to 7 days are presented in **Figure 6A**, **6B** and **6C**, respectively. P and Ca ion release profiles do not change significantly with copper loading in the first 24 h. However, clear differences can be seen in the release profiles of the following 7 days. In particular, the CPG copper-free glasses release the highest amount of P and Ca which then decreases with increasing the copper content. Decrease in P release could be related to the cross-linking effect of Cu^{2+} that makes the phosphate chains more interconnected, increasing their strength in solution. Decrease in Ca is expected as Ca^{2+} is replaced with Cu^{2+} in the synthesis. Release of Cu^{2+} ions clearly increases with copper content. Moreover, differently from the release of P and Ca, differences can be seen in the first 24 h, with CPG-Cu2 releasing less copper that CPG-Cu4 and CPG-Cu6.

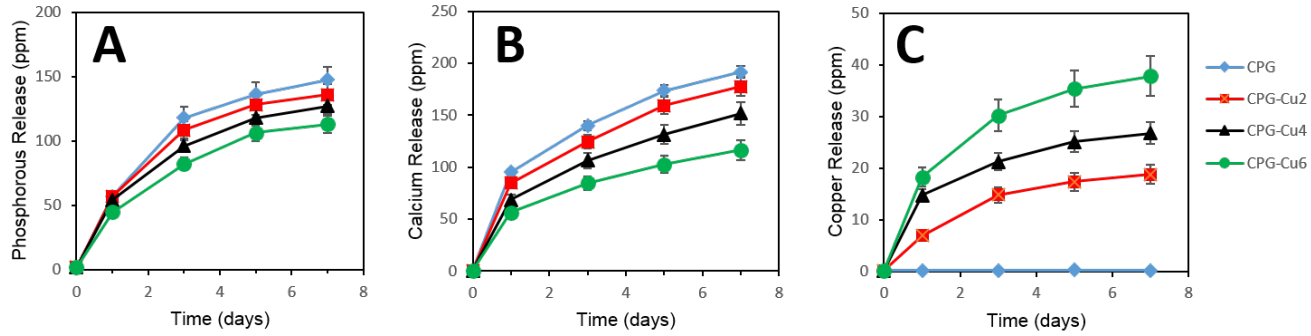

Figure 6. Release of phosphorus (A), calcium (B), and copper (C) in deionised water as a function of time for all glasses measured by ICP-OES.

3.7. Antimicrobial study

A quantitative ADM assay was performed on the dissolution products of the glasses when in contact with *S. aureus* strain for 7 days (**Figure 7**). In all the experiments, growth of *S. aureus* strain was used as a control. The bacterial viability is expressed as log10 CFU/mL (CFU = colony forming units) and error bars represent standard deviations (Two-way ANOVA for each time point). Three runs for each experiment were performed to validate the results found. As expected, the antibacterial activity increases with increasing Cu^{2+} content. CPG-Cu2 and CPG-Cu4 show a progressive reduction in the log10 of the mean number of viable counts from day 1 to 7. They show similar antibacterial activities at day 1 and day 3 when the reduction is statistically significant for both (1 log10 reduction, p value <0.017 at day 1 and 2 log10 reduction, p value >0.005 at day 3). At day 5 they both increase their antibacterial activity; however, the increase is much higher for CPG-Cu4 (more than 1 log10 reduction in the numbers of CFU compared to those for the control). Then the activity does not change until day 7. CPG-Cu6 glass is highly active even after

1 day of incubation, as it achieved a 5 log10 reduction, demonstrating a rapid bactericidal effect. Then, its activity increases up to day 3 (8 log10 reduction) and then stays constant at days 5 and 7. Interestingly, the undoped CPG sample shows a mild antibacterial activity that does not change over time. The same effect has been previously been observed in phosphate-based glasses prepared by MQ [43] and silicate-based glasses. [44] It has been suggested that this could be due to a change in pH values during glass degradation.

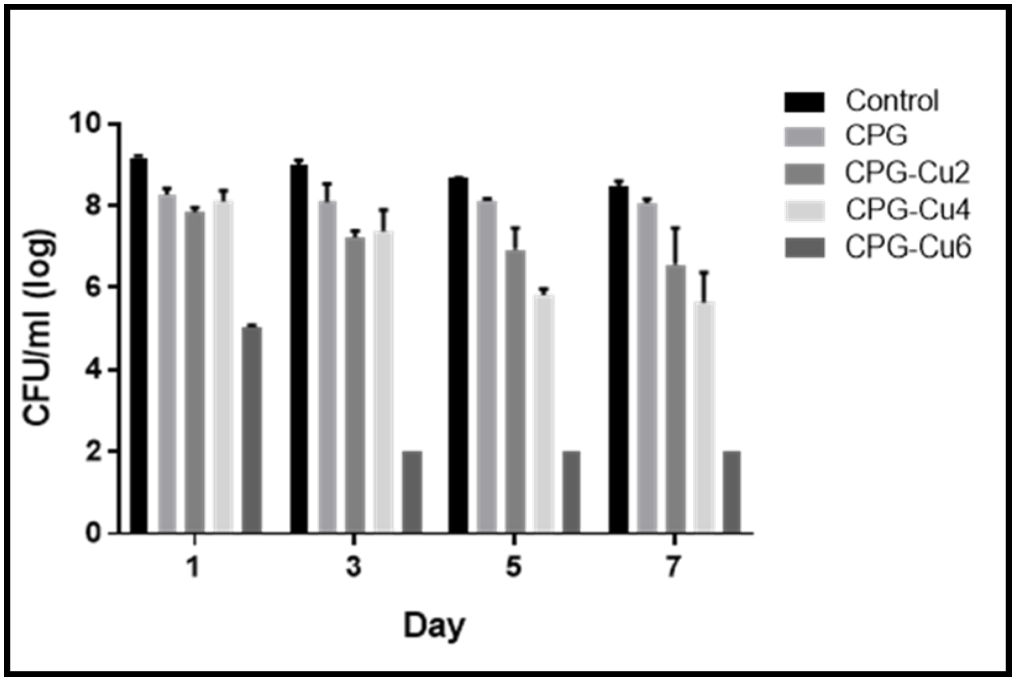

Figure 7. Antibacterial activity of all glasses against *S. aureus* expressed as the mean ± standard deviation (error bars). (****, $p < 0.0001$; ▲= minimum bacterial CFU/mL detection point).

3.8. In-vitro biocompatibility assessment

Biocompatibility of all glasses was assessed by evaluating attachment and viability of Saos-2 osteosarcoma cells cultured on their surfaces. These cells were selected because they possess

several osteoblastic features and they can therefore be used to mimic the osteoblast response to the glasses. [45, 46] Cell attachment was assessed via SEM and DAPI-Phalloidin staining. SEM images reported in **Figure 8** show that Saos-2 cells are attached and well spread on the surface of all glasses over a 5-day period. Cells form aggregates with flat morphology nicely attached over the surface of the glasses.

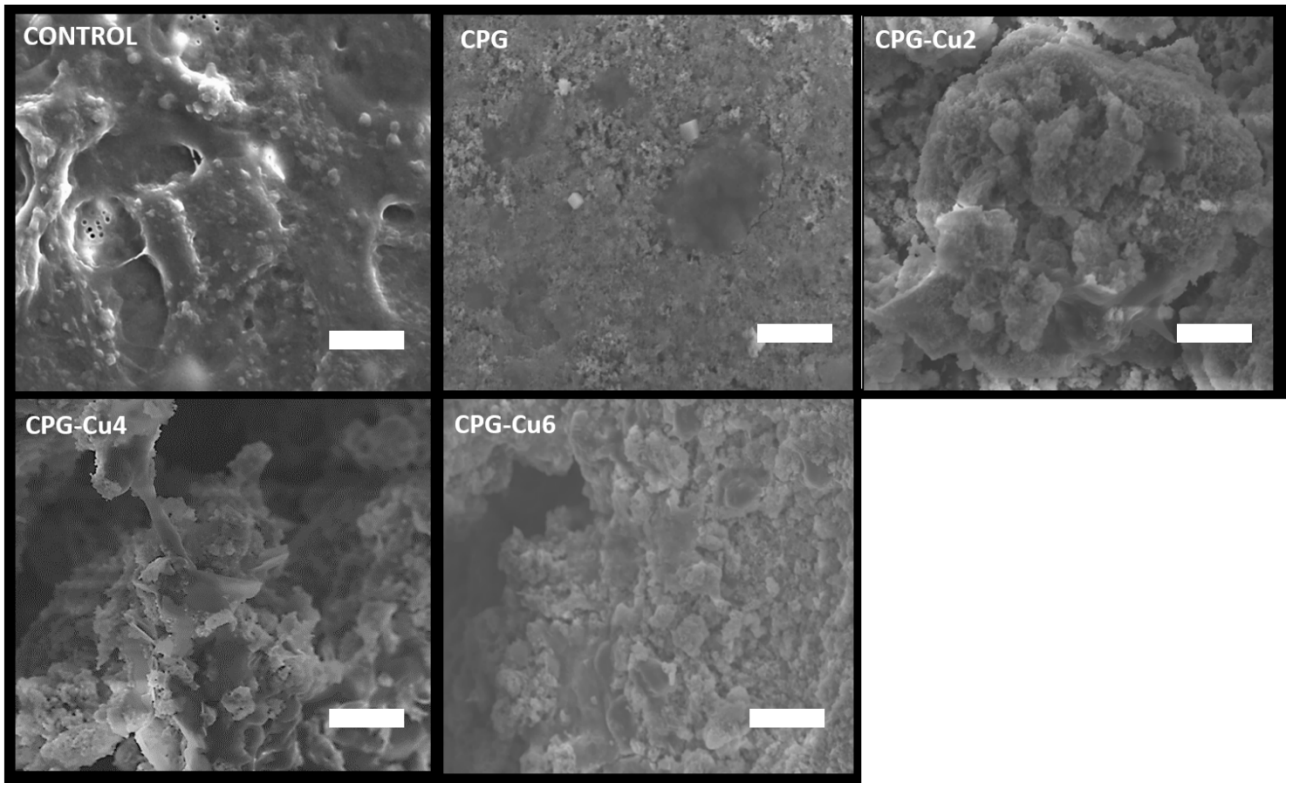

Figure 8. SEM images showing viability of Saos-2 cells when seeded onto the glasses after 5 days. Scale bar is 10 μm.

SEM results are confirmed by qualitative analysis based on DAPI- Phalloidin staining (**Figure 9**). Cells nuclei (blue) and filaments (green) show that cells are attached and spread on all glass surfaces after 5 days of seeding.

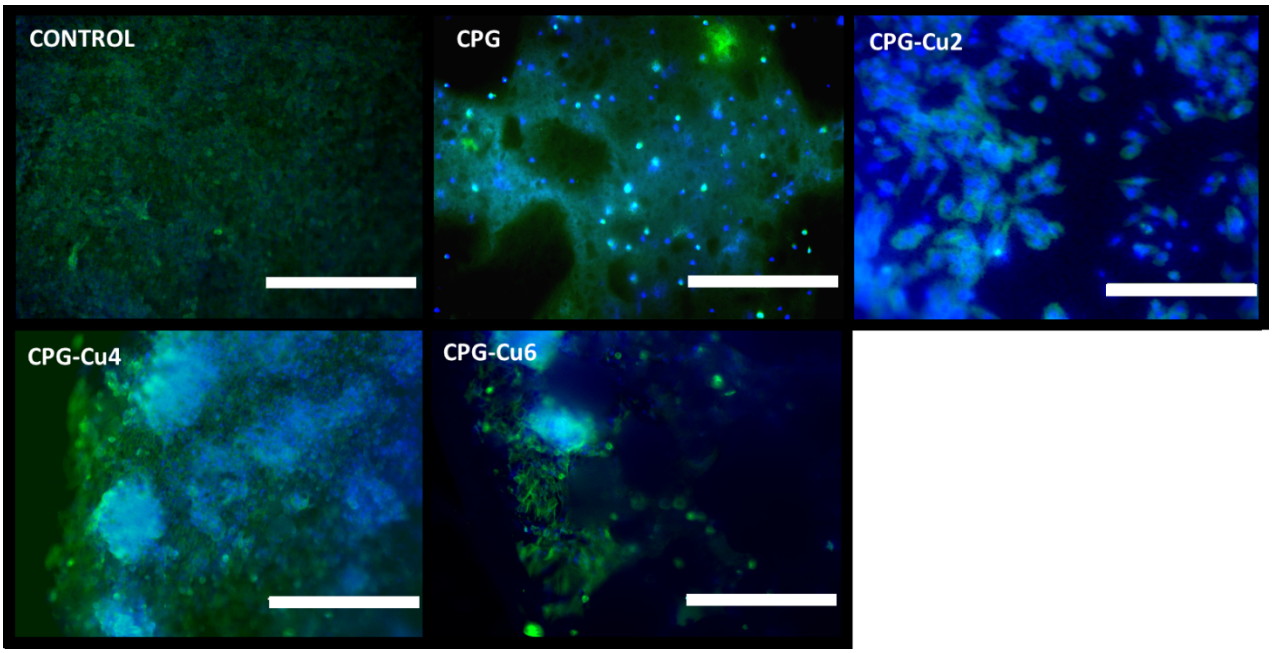

Figure 9. DAPI- Phalloidin staining of Saos-2 cells seeded onto the glasses after 5 days. The green fluorescent stain (phalloidin) shows filamentous actin and the blue (DAPI) shows nuclei. Scale bar is 400 μm.

Cell viability was then quantitatively assessed using the Alamar Blue assay. The graph shown in **Figure 10** represents the change in fluorescence of Alamar Blue dye as a direct indicator of cellular metabolic activity which is directly linked to the number of cells. Within each glass composition, cell growth does not change significantly from day 1 to day 3. However, from day 3 to day 5, all glasses show a significant increase in cell proliferation. The highest cell growth was observed for

the undoped sample CPG at day 5, which is very similar to the control. All Cu^{2+} doped samples also show high metabolic activity at day 5. However, their activity decreases as the Cu^{2+} content increases.

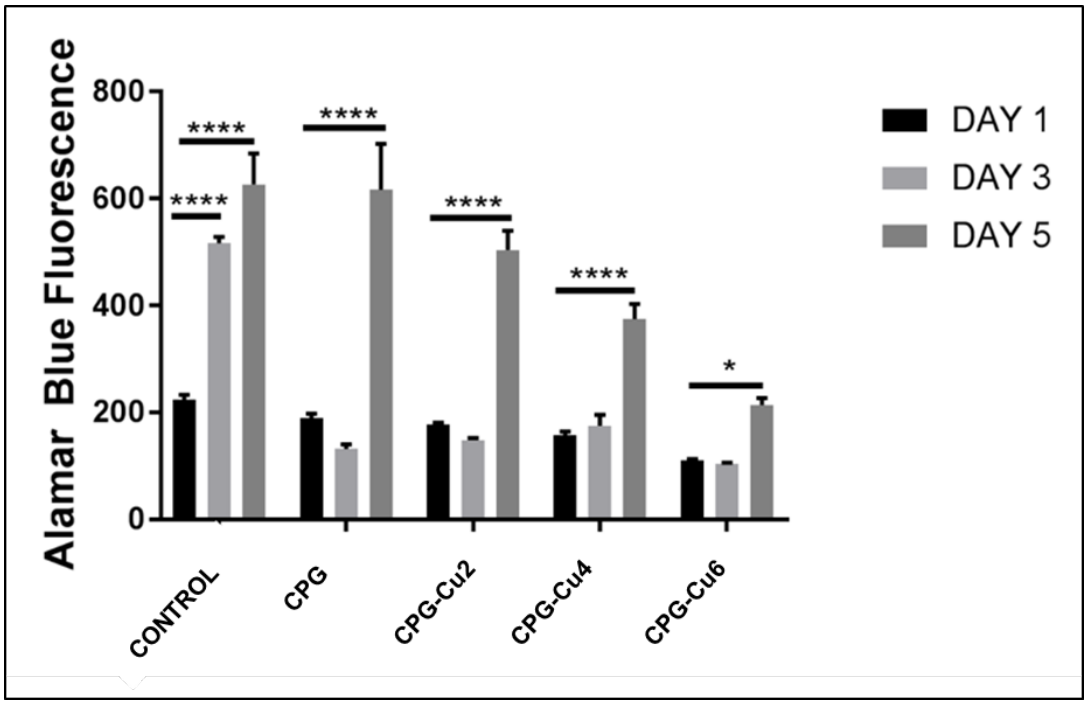

Figure 10. Cell viability measurement using the Alamar blue fluorescence assay after 1, 3, and 5 days in culture. Error bars are SD (n=3).

4. DISCUSSION

Calcium phosphate glasses have been widely investigated as multifunctional biomaterials capable of inducing bone tissue regeneration and simultaneously release of drug molecules in a controlled manner. However, the majority of the works presented so far refer to glasses prepared using the high temperature melt-quenching technique and in less extent using the sol-gel method. Moreover, very few studies refer to glasses doped with copper as an antibacterial ion. This study investigates

the structure, antibacterial activity and biocompatibility of copper-doped phosphate-based glasses prepared using a water-based, room temperature technique.

XRD patterns and DSC analysis show that all glasses are amorphous up to ~ 530 - 600 °C depending on the composition. Crystallisation temperatures are close to those reported for undoped phosphate glasses prepared via MQ (~ 450 - 650 °C) [7] and via SG (~ 500 °C). [47] Crystallisation of copper doped MQ fibres have also been reported around 500 - 550 °C. [18] The thermal stability of the systems prepared in this work is therefore comparable with that of MQ and SG ones.

^{31}P MAS NMR study has shown that in all glasses Q^1 is the predominant group. Predominance of Q^1-type groups is also confirmed by predominant bands which occur at 770 cm^{-1} and 1050 cm^{-1} in the Raman spectra. This is significantly different from the majority of bioresorbable calcium phosphate glasses presented in literature that have Q^2 as predominant group.

Species released from the glasses when immersed in water was monitored over a period of 7 days. The release of P and Ca followed a similar pattern, with very similar released occurring in the first 24 h for all compositions, followed by a progressive decrease of P and Ca release with increasing Cu content over 7 days. These results are in agreement with ^{31}P MAS NMR data as Cu^{2+} seems to decrease the dissolution rate of P and Ca, confirming the cross-linking effect. This shows that the degradation of the glasses can be tailored by optimising the addition of Cu^{2+} as a dopant. The amount of Cu^{2+} released increases with its content in agreement with Cu^{2+} release results reported on MQ phosphate glass fibres. [18] The same trend has been reported upon release of Zn^{2+} ions and Sr^{2+} from MQ phosphate glasses. [48, 49]

The antimicrobial effect of Cu^{2+} release was investigated against the gram positive bacteria *S.aureus*. It has to be noted that this is the first study on this kind being the previously reports limited to the antibacterial activity of phosphate-based glass fibres and bulk against *S. epidermidis*

[18, 51] and biofilms of *S. sanguis*. [51] Antimicrobial studies demonstrate a strong positive correlation between Cu^{2+} concentration/release and bactericidal properties. The glass that contains and releases the highest amount of Cu^{2+} (CPG-Cu6) was shown to be the most effective in killing the bacteria reducing significantly the number of viable bacteria from day 1 (5 log reduction). The activity of CPG-Cu2 and CPG-Cu4 was also significant but mainly at day 5.

Cytocompatibility assessment was carried out by putting in contact all synthesised glasses with Saos-2 osteosarcoma cells for a period of 5 days. Quantitative and qualitative analysis showed that copper-doped glasses were able to support attachment and expansion of Saos-2 cells. In particular, cell viability increases significantly at day 5 for all compositions. Same trend has been previously observed in Cu^{2+} doped silicate-based glasses. [51] It has to be noted that a decrease in cell viability was observed with increasing Cu^{2+} concentration. This could be explained with the fact that high doses of Cu^{2+} increase the reactive oxygen species leading to a decrease in cell viability. [51] On the basis of these results, a Cu amount of 2 mol % seems to be the optimal composition for bone tissue engineering applications; CPG-Cu2 has been shown to deliver good antibacterial activity and simultaneously induce significant cell proliferation and growth at day 5.

5. CONCLUSIONS

In this study a series of calcium phosphate glasses doped with 0, 2, 4 and 6 mol% of Cu^{2+} have been successfully synthesised using a room temperature, aqueous route. All samples prepared showed a good thermal stability being amorphous up to ~ 530 - 600 °C depending on the copper content. ^{31}P MAS NMR and Raman spectroscopy have shown that the glasses are mainly formed by Q^1 groups, with Q^2 groups observed only in the 4 and 6 mol% Cu^{2+} doped glasses. Dissolution studies have shown that P release decreases with increasing Cu^{2+} content, suggesting a cross-

linking effect of Cu^{2+} between phosphate chains, which is also supported by ^{31}P MAS NMR results. Calcium release also decreases with Cu^{2+} content due to the replacement of Ca^{2+} with Cu^{2+} during synthesis whilst Cu^{2+} release increases, as expected. The antibacterial activity of the glasses against *S. aureus* is dose dependent, as increases with Cu^{2+} content. In particular, the glass containing 6 mol% of Cu^{2+} shows significant activity even after 1 day of incubation. Cytocompatibility studies have shown that osteoblast-like cells Saos-2 attach and spread on the surface of all glasses over a period of 5 days. Results have shown that viability of cells increase from day 1 to day 5 for all glass compositions, even if a decrease in cell viability is observed with increasing Cu^{2+} content. To conclude, this study has shown that copper-doped calcium phosphate glasses prepared using a mild, aqueous based technique can be used as bioresorbable materials to prevent post-surgical infections and bone tissue regeneration.

6. SUPPORTING INFORMATION AVAILABLE

The following files are available free of charge: XRD patterns of all glasses after calcination at 200, 400 and 700 °C.

7. ACKNOWLEDGMENTS

The authors would like to acknowledge EPSRC (grant EP/P033636/1) and Royal Society (grant RSG\R1\180191) for providing the funding to conduct this study. The authors are also grateful to Dr D. Jones and Miss A. M Nelson for their help with the SEM/EDX and Dr G. Palmer for his help with ICP-OES measurements. DC thanks the Doctoral College, University of Surrey and Fourth State Medicine Ltd for funding Mr Nikolaou PhD studentship.

JVH thanks EPSRC, the University of Warwick and the Birmingham Science City Program for partial funding of the solid state NMR infrastructure at Warwick. The latter program accessed the Birmingham Science City Advanced Materials Project 1: Creating and Characterising Next Generation Advanced Materials, which derived support from Advantage West Midlands (AWM) and the European Regional Development Fund (ERDF). NLK thanks EPSRC for a PhD studentship through the EPSRC Centre for Doctoral Training in Molecular Analytical Science, grant number EP/L015307/1.

REFERENCES

(1) Abou Neel, E. A.; Pickup, D. M.; Valappil, S. P.; Newport, R. J.; Knowles, J. C. Bioactive Functional Materials: A Perspective on Phosphate-Based Glasses. *J. Mater. Chem.* **2009**, *19* (6), 690–701.

(2) Islam, M. T.; Felfel, R. M.; Abou Neel, E. A.; Grant, D. M.; Ahmed, I.; Hossain, K. M. Z. Bioactive Calcium Phosphate–Based Glasses and Ceramics and Their Biomedical Applications: A Review. *J. Tissue Eng.* **2017**, *8*, 1–16.

(3) Knowles, J. C. Phosphate Based Glasses for Biomedical Applications. *J. Mater. Chem.* **2003**, *13* (10), 2395.

(4) Grover, L. M.; Wright, A. J.; Gbureck, U.; Bolarinwa, A.; Song, J.; Liu, Y.; Farrar, D. F.; Howling, G.; Rose, J.; Barralet, J. E. The Effect of Amorphous Pyrophosphate on Calcium Phosphate Cement Resorption and Bone Generation. *Biomaterials* **2013**, *34* (28), 6631–6637.

(5) Lapa, A.; Cresswell, M.; Jackson, P.; Boccaccini, A. R.; Lapa, A.; Cresswell, M.; Jackson, P.; Boccaccini, A. R.; Lapa, A.; Cresswell, M. Phosphate Glass Fibres with Therapeutic

Ions Release Capability – a Review Phosphate Glass Fi Bres with Therapeutic Ions Release Capability – a Review. *Adv. Appl. Ceram.* **2019**, 1–14.

(6) Bitar, M.; Salih, V.; Mudera, V.; Knowles, J. C.; Lewis, M. P. Soluble Phosphate Glasses: In Vitro Studies Using Human Cells of Hard and Soft Tissue Origin. *Biomaterials* **2004**, *25* (12), 2283–2292.

(7) Ahmed, I.; Lewis, M.; Olsen, I.; Knowles, J. C. Phosphate Glasses for Tissue Engineering: Part 1. Processing and Characterisation of a Ternary-Based P_2O_5-CaO-Na_2O Glass System. *Biomaterials* **2004**, *25* (3), 491–499.

(8) Al Qaysi, M.; Walters, N. J.; Foroutan, F.; Owens, G. J.; Kim, H. W.; Shah, R.; Knowles, J. C. Strontium- and Calcium-Containing, Titanium-Stabilised Phosphate-Based Glasses with Prolonged Degradation for Orthopaedic Tissue Engineering. *J. Biomater. Appl.* **2015**.

(9) Carta, D.; Pickup, D. M.; Knowles, J. C.; Smith, M. E.; Newport, R. J. Sol–Gel Synthesis of the P_2O_5-CaO-Na_2O-SiO_2 System as a Novel Bioresorbable Glass. *J. Mater. Chem.* **2005**, *15*, 2134–2140.

(10) Carta, D.; Pickup, D. M.; Knowles, J. C.; Ahmed, I.; Smith, M. E.; Newport, R. J. A Structural Study of Sol-Gel and Melt-Quenched Phosphate-Based Glasses. *J. Non. Cryst. Solids* **2007**, *353*, 1759–1765.

(11) Carta, D.; Knowles, J. C.; Smith, M. E.; Newport, R. J. Synthesis and Structural Characterization of P_2O_5-CaO-Na_2O Sol-Gel Materials. **2007**, *353*, 1141–1149.

(12) Pickup, D. M.; Newport, R. J.; Knowles, J. C. Sol–Gel Phosphate-Based Glass for Drug Delivery Applications. *J. Biomater. Appl.* **2012**, *26* (5), 613–622.

(13) Foroutan, F.; Walters, N. J.; Owens, G. J.; Mordan, N. J.; Kim, H.-W.; de Leeuw, N. H.; Knowles, J. C. Sol-Gel Synthesis of Quaternary $(P_2O_5)_{55}$-$(CaO)_{25}$-$(Na_2O)_{(20-x)}$-$(TiO_2)_x$

Bioresorbable Glasses for Bone Tissue Engineering Applications (x = 0, 5, 10, or 15). *Biomed. Mater.* **2015**.

(14) Soulié, J.; Gras, P.; Marsan, O.; Laurencin, D.; Rey, C.; Combes, C. Development of a New Family of Monolithic Calcium (Pyro)Phosphate Glasses by Soft Chemistry. *Acta Biomater.* **2016**, *41*, 320–327.

(15) Gras, P.; Rey, C.; Marsan, O.; Sarda, S.; Combes, C. Synthesis and Characterisation of Hydrated Calcium Pyrophosphate Phases of Biological Interest. *Eur. J. Inorg. Chem.* **2013**, *2013* (34), 5886–5895.

(16) Pickup, D. M.; Ahmed, I.; FitzGerald, V.; Moss, R. M.; Wetherall, K. M.; Knowles, J. C.; Smith, M. E.; Newport, R. J. X-Ray Absorption Spectroscopy and High-Energy XRD Study of the Local Environment of Copper in Antibacterial Copper-Releasing Degradable Phosphate Glasses. *J. Non. Cryst. Solids* **2006**, *352* (28–29), 3080–3087.

(17) Mulligan, A. M.; Wilson, M.; Knowles, J. C. The Effect of Increasing Copper Content in Phosphate-Based Glasses on Biofilms of Streptococcus Sanguis. *Biomaterials* **2003**, *24* (10), 1797–1807.

(18) Abou Neel, E. A.; Ahmed, I.; Pratten, J.; Nazhat, S. N.; Knowles, J. C. Characterisation of Antibacterial Copper Releasing Degradable Phosphate Glass Fibres. *Biomaterials* **2005**.

(19) Mishra, A.; Petit, L.; Pihl, M.; Andersson, M.; Salminen, T.; Rocherullé, J.; Massera, J. Thermal, Structural and in Vitro Dissolution of Antimicrobial Copper-Doped and Slow Resorbable Iron-Doped Phosphate Glasses. *J. Mater. Sci.* **2017**, *52* (15), 8957–8972.

(20) Rath, S. N.; Brandl, A.; Hiller, D.; Hoppe, A.; Gbureck, U.; Horch, R. E.; Boccaccini, A. R.; Kneser, U. Bioactive Copper-Doped Glass Scaffolds Can Stimulate Endothelial Cells in Co-Culture in Combination with Mesenchymal Stem Cells. *PLoS One* **2014**, *9* (12), 1–24.

(21) Rodriguez, P. J.; Gonzalez, M.; Rios, S. Modulation of the Proliferation and Differentiation of Human Mesenchymal Stem Cells by Copper. *J. Cell. Biochem.* **2002**, *85*, 92–100.

(22) Li, J.; Zhai, D.; Lv, F.; Yu, Q.; Ma, H.; Yin, J.; Yi, Z.; Liu, M.; Chang, J.; Wu, C. Preparation of Copper-Containing Bioactive Glass/Eggshell Membrane Nanocomposites for Improving Angiogenesis, Antibacterial Activity and Wound Healing. *Acta Biomater.* **2016**, *36*, 254–266.

(23) Luca, M.; Pietro, S.; Davide, C.; Ravaioli, S.; Cangini, I.; Pietrocola, G.; Sandro, G.; Arciola, C. R. Scenery of Staphylococcus Implant Infections in Orthopedics. *Futur. Microbioligy* **2011**, *6* (11), 1329–1349.

(24) Abou Neel, E. A.; Knowles, J. C. Physical and Biocompatibility Studies of Novel Titanium Dioxide Doped Phosphate-Based Glasses for Bone Tissue Engineering Applications. *J. Mater. Sci. Med.* **2008**, *19* (1), 377–386.

(25) Qaysi, M. Al; Petrie, A.; Shah, R.; Knowles, J. C. Degradation of Zinc Containing Phosphate-Based Glass as a Material for Orthopedic Tissue Engineering. *J. Mater. Sci. Mater. Med.* **2016**, *27* (10), 157.

(26) Salih, V.; Franks, K.; James, M.; Hastings, G. W.; Knowles, J. C.; Olsen, I. Development of Soluble Glasses for Biomedical Use Part II: The Biological Response of Human Osteoblast Cell Lines to Phosphate-Based Soluble Glasses. *J. Mater. Sci. Med.* **2000**, *11* (10), 615–620.

(27) Abou Neel, E. A.; Chrzanowski, W.; Pickup, D. M.; O'Dell, L. A.; Mordan, J. N.; Newport, R. J.; Smith, M. E.; Knowles, J. Structure and Properties of Strontium-Doped Phosphate-Based Glasses. *J R Soc Interface* **2009**, *6*, 435–446.

(28) Ahmed, I.; Parsons, A.; Jones, A.; Walker, G.; Scotchford, C.; Rudd, C. Cytocompatibility

and Effect of Increasing MgO Content in a Range of Quaternary Invert Phosphate-Based Glasses. *J. Biomater. Appl.* **2010**, *24* (6), 555–575.

(29) Gough, J. E.; Christian, P.; Scotchford, C. A.; Rudd, C. D.; Jones, I. A. Synthesis , Degradation , and in Vitro Cell Responses of Sodium Phosphate Glasses for Craniofacial Bone Repair. *J. Biomed. Mater. Res.* **2002**, *59*, 481–489.

(30) Slater, C.; Laurencin, D.; Burnell, V.; Smith, M. E.; Grover, L. M.; Hriljac, J. A.; Wright, A. J. Enhanced Stability and Local Structure in Biologically Relevant Amorphous Materials Containing Pyrophosphate. *J. Mater. Chem.* **2011**, *21* (46), 18783.

(31) Massiot, D.; Fayon, F.; Capron, M.; King, I.; Le Calvé, S.; Alonso, B.; Durand, J.-O.; Bujoli, B.; Gan, Z.; Hoatson, G. Modelling One- and Two-Dimensional Solid-State NMR Spectra. *Magn. Reson. Chem.* **2002**, *40* (1), 70–76.

(32) Gutierrez, J.; Barry-Ryan, C.; Bourke, P. Antimicrobial Activity of Plant Essential Oils Using Food Model Media: Efficacy, Synergistic Potential and Interactions with Food Components. *Food Microbiol.* **2009**, *26* (2), 142–150.

(33) Stedman, A.; Maluquer De Motes, C.; Lesellier, S.; Dalley, D.; Chambers, M.; Gutierrez-Merino, J. Lactic Acid Bacteria Isolated from European Badgers (Meles Meles) Reduce the Viability and Survival of Bacillus Calmette-Guerin (BCG) Vaccine and Influence the Immune Response to BCG in a Human Macrophage Model. *BMC Microbiol.* **2018**.

(34) Eliaz, N.; Metoki, N. Calcium Phosphate Bioceramics : A Review of Their History, Structure, Properties, Coating Technologies and Biomedical Applications. *Materials (Basel).* **2017**, *10* (334), 2–104.

(35) Slater, C.; Laurencin, D.; Burnell, V.; Smith, M. E.; Grover, L. M.; Hriljac, J. A.; Wright, A. J. Enhanced Stability and Local Structure in Biologically Relevant Amorphous Materials

Containing Pyrophosphate. *J. Mater. Chem.* **2011**, *21*, 18783.

(36) Navarro, M.; Del Valle, S.; Martínez, S.; Zeppetelli, S.; Ambrosio, L.; Planell, J. A.; Ginebra, M. P. New Macroporous Calcium Phosphate Glass Ceramic for Guided Bone Regeneration. *Biomaterials* **2004**.

(37) Abrahams, I.; Franks, K.; Hawkes, G. E.; Philippou, G.; Knowles, J.; Nunes, T. 23Na, 27Al and 31P NMR and X-Ray Powder Diffraction Study of Na/Ca/Al Phosphate Glasses and Ceramics. *J. Mater. Chem.* **1997**, *7* (23), 1573–1580.

(38) Gras, P.; Baker, A.; Combes, C.; Rey, C.; Sarda, S.; Wright, A. J.; Smith, M. E.; Hanna, J. V.; Gervais, C.; Laurencin, D.; et al. From Crystalline to Amorphous Calcium Pyrophosphates: A Solid State Nuclear Magnetic Resonance Perspective. *Acta Biomater.* **2016**, *31*, 348–357.

(39) Brow, R. K.; Tallant, D. R.; Myers, S. T.; Phifer, C. C. The Short-Range Structure of Zinc Polyphosphate Glass. *J. Non. Cryst. Solids* **1995**, *191* (5), 45–55.

(40) Pemberton, J. E.; Latifzadeh, L.; Fletcher, J. P.; Risbud, S. H. Raman Spectroscopy of Calcium Phosphate Glasses with Varying CaO Modifier Concentrations. *Chem. Mater.* **1991**, *3* (13), 195–200.

(41) Lai, Y. M.; Liang, X. F.; Yang, S. Y.; Wang, J. X.; Cao, L. H.; Dai, B. Raman and FTIR Spectra of Iron Phosphate Glasses Containing Cerium. *J. Mol. Struct.* **2011**, *992* (1–3), 84–88.

(42) Stoch, P.; Szczerba, W.; Bodnar, W.; Ciecinska, M.; Stoch, A.; Burkel, E. Structural Properties of Iron-Phosphate Glasses: Spectroscopic Studies and Ab Initio Simulations. *Phys. Chem. Chem. Phys.* **2014**, *16*, 19917–19927.

(43) Valappil, S. P.; Ready, D.; Abou Neel, E. A.; Pickup, D. M.; Chrzanowski, W.; O'Dell, L.

A.; Newport, R. J.; Smith, M. E.; Wilson, M.; Knowles, J. C. Antimicrobial Gallium-Doped Phosphate-Based Glasses. *Adv. Funct. Mater.* **2008**, *18* (5), 732–741.

(44) Begum, S.; Johnson, W. E.; Worthington, T.; Martin, R. A. The Influence of PH and Fluid Dynamics on the Antibacterial Efficacy of 45S5 Bioglass. *Biomed. Mater.* **2016**, *11* (1), 015006.

(45) Rana, K. S.; Souza, L. P. De; Isaacs, M. A.; Raja, F. N. S.; Morrell, A. P.; Martin, R. A. Development and Characterization of Gallium-Doped Bioactive Glasses for Potential Bone Cancer Applications. *ACS Biomater. Sci. Eng.* **2017**, *3* (12), 3425–3432.

(46) Rodan, S. B.; Imai, Y.; Thiede, M. A.; Wesolowski, G.; Thompson, D.; Bar-shavit, Z.; Shull, S.; Mann, K.; Rodan, G. A. Characterization of a Human Osteosarcoma Cell Line (Saos-2) with Osteoblastic Properties. *Cancer Res.* **1987**, *47*, 4961–4966.

(47) Pickup, D. M.; Guerry, P.; Moss, R. M.; Knowles, J. C.; Smith, M. E.; Newport, R. J. New Sol–Gel Synthesis of a $(CaO)_{0.3}(Na_2O)_{0.2}(P_2O_5)_{0.5}$ Bioresorbable Glass and Its Structural Characterisation. *J. Mater. Chem.* **2007**, *17* (45), 4777.

(48) Raja, F. N. S.; Worthington, T.; Isaacs, M. A.; Rana, K. S.; Martin, R. A. The Antimicrobial Efficacy of Zinc Doped Phosphate-Based Glass for Treating Catheter Associated Urinary Tract Infections. *Mater. Sci. Eng. C* **2019**, *103*, 109868.

(49) Al Qaysi, M.; Walters, N. J.; Foroutan, F.; Owens, G. J.; Kim, H.-W.; Shah, R.; Knowles, J. C. Strontium- and Calcium-Containing, Titanium-Stabilised Phosphate-Based Glasses with Prolonged Degradation for Orthopaedic Tissue Engineering. *J. Biomater. Appl.* **2015**, *30* (3), 300–310.

(50) Qaysi, M. Al; Walters, N. J.; Foroutan, F.; Owens, G. J.; Kim, H.; Shah, R.; Knowles, J. C. Strontium- and Calcium-Containing , Glasses with Prolonged Degradation for Orthopaedic

Tissue Engineering. **2015**, *30* (3), 300–310.

(51) Catherine, G.; Bordeleau, L.; Barralet, J.; Doillon, C. J. Biomaterials The Stimulation of Angiogenesis and Collagen Deposition by Copper. *Biomaterials* **2010**, *31*, 824–831.

FOR TABLE OF CONTENTS ONLY

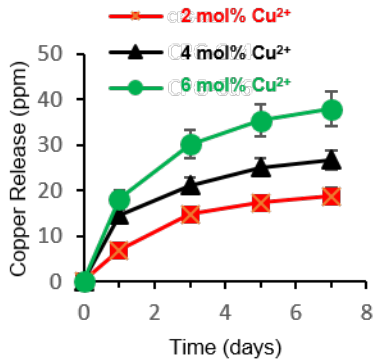

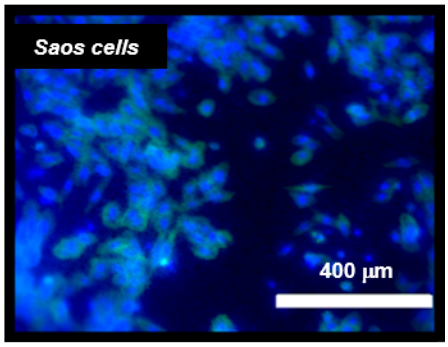

SUPPORTING INFORMATION

Antibacterial Copper-Doped Calcium Phosphate Glasses for Bone Tissue Regeneration

Farzad Foroutan,†,‡ Jamie McGuire,†,‡ Priyanka Gupta,§ Athanasios Nikolaou,‡ Benjamin A. Kyffin,‡ Nicole L. Kelly,⊥ John V. Hanna,⊥ Jorge Gutierrez-Merino,‖ Jonathan C. Knowles,#,□,○,∆ Song-Yi Baek,# Eirini Velliou,§ and Daniela Carta*,‡

‡Department of Chemistry, §Department of Chemical and Process Engineering, Bioprocess and Biochemical Engineering group (BioProChem), ‖School of Biosciences and Medicine, University of Surrey, Guildford GU2 7XH, United Kingdom

⊥Department of Physics, University of Warwick, Coventry CV4 7AL, United Kingdom

#Division of Biomaterials and Tissue Engineering, Eastman Dental Institute, University College London, 256 Gray's Inn Road, 10 London WC1X 8LD, United Kingdom

□The Discoveries Centre for Regenerative and Precision Medicine, University College London, London WC1E 6BT, United Kingdom

○Department of Nanobiomedical Science & BK21 PLUS NBM Global Research Center for Regenerative Medicine, and ∆UCL Eastman−Korea Dental Medicine Innovation Centre, Dankook University, Cheonan 31114, Republic of Korea

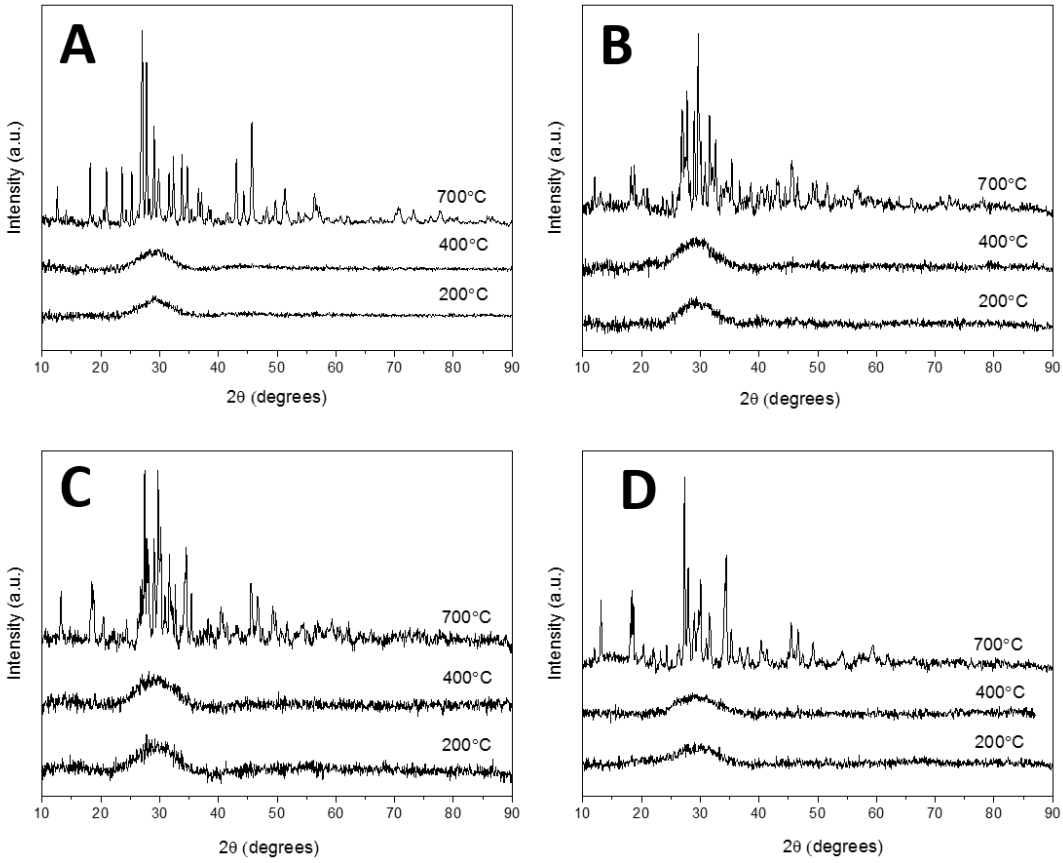

Figure S1: X-ray diffraction patterns of A): CPG; B): CPG-Cu2; C): CPG-Cu4; D) CPG-Cu6.